Design of dense InP based optical antenna array for 2D beam steering

Fathema Farjana, Yi Wang, and Yuqing Jiao

Eindhoven Hendrik Casimir Institute (EHCI), Eindhoven University of Technology, Eindhoven, 5600MB, the Netherlands

This paper presents an optical phased array (OPA) utilizing SiO_2 gratings on InP membrane on Silicon (IMOS) platform for large-angle optical beam steering. Width-engineered waveguides are leveraged for crosstalk suppression to achieve dense integration. In the simulation, < -20 dB channel crosstalk is achieved at 1550 nm wavelength for a 2 mm-long antenna array with 1 µm pitch. A large steering range of 73° × 13.6° is obtained with an SNR of -7.4 dB. Such a 2D steering OPA has great potential to realize full-solid LiDAR for its large FOV, small SNR, and monolithic compatibility with InP lasers and amplifiers.

Introduction:

Optical phased array (OPA) has become a crucial candidate for light detection and ranging (LiDAR) in autonomous driving cars for its potential of precise, ultrafast inertia-free beam steering of high reliability, high scalability, and mass manufacturability[1]. OPA in automotive cars needs to achieve a large FoV and high resolution. However, the desirable wide FoV is limited by the evanescent coupling in an antenna array, and the coupling strength is inversely proportional to the antenna spacing [1]. A sparse array with non-uniform emitter spacing provides an interesting alternative to reduce the crosstalk. Though this scheme keeps the side lobes suppressed during the beam-steering process while achieving 80° × 17° FoV, it sacrifices the energy concentration in the main lobe (≤ 40% [2]). For long-range applications like in LiDAR, it could be detrimental as it will result in the degradation of signal-to-noise ratio (SNR). Alternatively, an ultra-compact dense array with subwavelength pitch has been proposed with very low crosstalk (below< -18 dB) using thin waveguide strips [3] and also by using periodic nano-blocks [4]. However, in these designs, the width of nano blocks[4] and the minimum gap [3] of a few tens of nanometers, are challenging in fabrication. Song W. et al. has proposed a superlattice structure of waveguides at sub-wavelength-pitch, where the crosstalk between adjacent waveguides can be suppressed under -20 dB by changing the widths of the waveguides [5]. This superlattice concept is leveraged in this paper to suppress crosstalk.

For Si photonic-based LiDAR systems, it is still challenging to realize the monolithic integration of laser source and semiconductor optical amplifier (SOA) arrays which are important for a beam steerer [6]. In contrast, the InP membrane on silicon (IMOS) platform can provide monolithic integration of active and passive devices and the compactness of SOI platform [7]. In this paper, high-density integration of OPA is achieved on the IMOS platform using superlattice theory for crosstalk suppression. For the eye-safe wavelength range of 1500-1600 nm, the design resulted in a high lateral FoV for 2D beam steering with low SNR.

Design:

The structure of the OPA on the IMOS platform is shown in Fig. 1. The gratings are on top of a 300 nm thick InP membrane waveguiding layer as shown in Fig 1(a). The buffer layer for IMOS platform is composed of benzocyclobutene (BCB) and SiO_2 stacks [8], but in the design it is approximated with 2 µm layer of SiO_2, since the BCB layer do not interact with the optical mode [6]. The low-index-contrast SiO_2 gratings are designed on the surface of the highly confined InP membrane waveguide as proposed in [6] to achieve weak coupling. A thickness of 200 nm is chosen for the gratings to ensure about 90% of the light is emitted from the grating antenna by 2 mm effective length. This 2 mm effective length is long enough to produce a beam of high resolution as proven in [6]. To overcome the crosstalk throughout the designed array the superlattice concept is used where the array is composed of subarrays of waveguides. In the subarray, the cross-talk is minimized between adjacent waveguides by introducing propagation constant mismatch using different waveguides widths. The subarrays are made sufficiently large to avoid crosstalk among same width waveguides. In the schematic of Fig. 1(b) the grating array superlattice is composed of N number of subarrays. Fig 1(c) shows that, each subarray of the design consists of two antennas of widths W1 = 550 nm and W2 = 580 nm, and grating periods of Λ_1 and Λ_2 of 50% duty cycle respectively. Here in the design for a pitch of 1 µm, a 30 nm width mismatch is used in the subarray that created an effective index mismatch of 0.04 to suppress the crosstalk between adjacent antennas. Fig. 1(d) depicted the 3D structure of the design. In our design, the longitudinal beam steering (θ, along the antenna length) is done by wavelength tuning. Since in a subarray, two widths are used, the effective index (n_{eff}) of each grating is also different. This leads to different periods of the antennas in the subarray in order to achieve a same emission angle. In the design the emission angle θ is chosen 13° for 1550 nm central wavelength (λ_0) to prevent the Bragg reflection. The grating periods (Λ) are calculated for different widths based on their effective indices using the grating equation [6]:

Finally, we obtain Λ_1 = 726 nm and Λ_2 = 713 nm for 550 and 580 nm antenna widths, respectively.

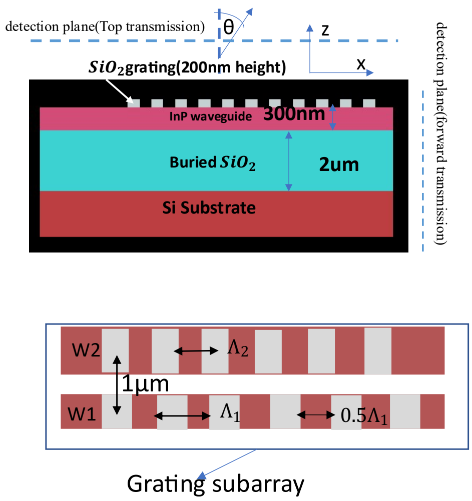

(a) (b)

(c) (d)

Figure 1. (a): Layer structure of grating antenna on IMOS platform, (b): Schematic of the grating sub-array, (c): Grating antenna subarray structure, (d): 3D illustration of grating based OPA.

Simulation:

As 3D finite-difference time-domain (FDTD) algorithm is computationally heavy for large structures, the crosstalk of the design is verified using Lumerical's Eigen Mode Expansion (EME) solver. A 2 mm antenna length is calculated for a 0.05° target angular resolution [6]. A simplified model is shown in Fig. 2(a) to study the crosstalk of a superlattice array of two alternating widths, where three waveguide is simulated (on which the gratings are made). The 1st (WG1) and 3rd (WG3) waveguides are of same width of 550 nm and 2nd (WG2) waveguide is of 580 nm. In the simulation, TE mode is chosen for the WGs. Fig. 2(b) shows that, the launched light in WG1 have minimal interaction with the adjacent waveguide resulting in crosstalk < -20 dB depicted in line graph of Fig. 2(c). To compare the result with equal-width WGs Fig. 2(b) illustrates the field profile where a strong coupling can be seen in neighboring WGs making it unsuitable for the array design.

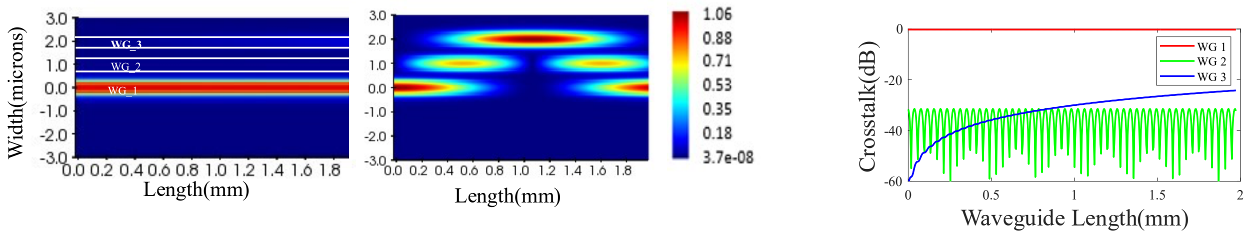

(a) (b) (c)

Figure 2. (a): Field profile for array of 3 WGs of 550 and 580 nm width. (b): Field profile for same width (550 nm) WG array showing strong field overlap. (c): Line-graph of crosstalk in WG2 and WG3 from source waveguide WG1.

The designed array is a 1D array consisting of 8 subarrays of two different widths antenna with extra one of 580 nm width to make the structure symmetric around the middle antenna. The steering angle and FWHM (full width at half maximum) of the beam in the far field are recorded for these two GA widths by changing the wavelength from 1500-1600 nm in 20 nm steps. Here, to reduce the simulation time, only 40 nm length is simulated. As scattering is a linear process, the FWHM of a full 2 mm long device can be obtained via extrapolation. In simulation, A total of 13.6° of steering angle is achieved for a wavelength tuning range of 100 nm with an average beam width of ~2.35° and ~2.41° for 550 and 580 nm GA, respectively. The steering angle and FWHM for both the GA are in good agreement, as shown in Fig 3(a). Fig. 3(b) depicts the longitudinal steering of 13.6° with beam intensity for the 1×17 channels array for the 100 nm wavelength range. For 40 um length of the antenna, the array achieved an average beam width of 2.351°. Here, the beam intensity decreases slightly with increasing steering wavelength.

a) (b)

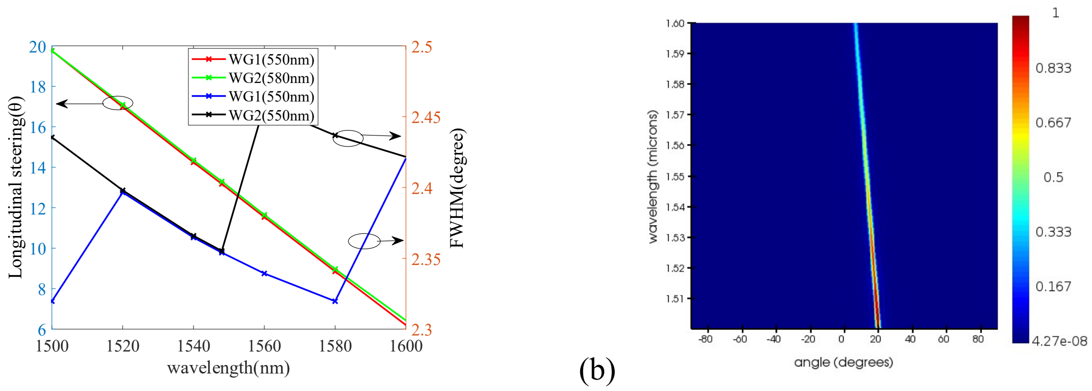

Figure 3: (a): Steering angle with wavelength and FWHM beam width of the steered beam of 550 and 580 nm GA. (b): Wavelength steered map for 100 nm wavelength range and steering intensity.

Now, to see the steering capability in the lateral direction (ψ, across the antenna array) of the 17 channels array, the beam is steered by changing the phase shift between adjacent antennas from -140° to +140° for the 1550 nm wavelength. In Fig. 4(a) the steering map is shown where a FoV of 73° is achieved in the lateral direction with side lobe suppression ratio (SLSR) of -7.4 dB. Here, the beam intensity is normalized to 1 and the pattern envelope is conserved. The beam width is limited by the diffraction from array size of 17 channels to 4.58°. It is also seen in the figure that the beam width of main lobe has broadened to 5.73° when steered to the edge. By combing lateral steering with the wavelength tuning, 2D beam steering with 1 × 17 channels GA array is achieved. Here for longitudinal steering, the wavelength is tuned from 1500-1600 nm, and lateral steering is done by changing the phase from -140° to 140°. In Fig. 4(b), this 2D steering map is shown. The beam is steered along the perimeter of the entire field of view of 73 ° × 13.6° in ψ × θ. The normalized intensity of far-fields of these steered beams are shown overlaid upon each other, and the dotted rectangular area shows the entire FoV. In the figure, the respective steering values for beam positions are shown.

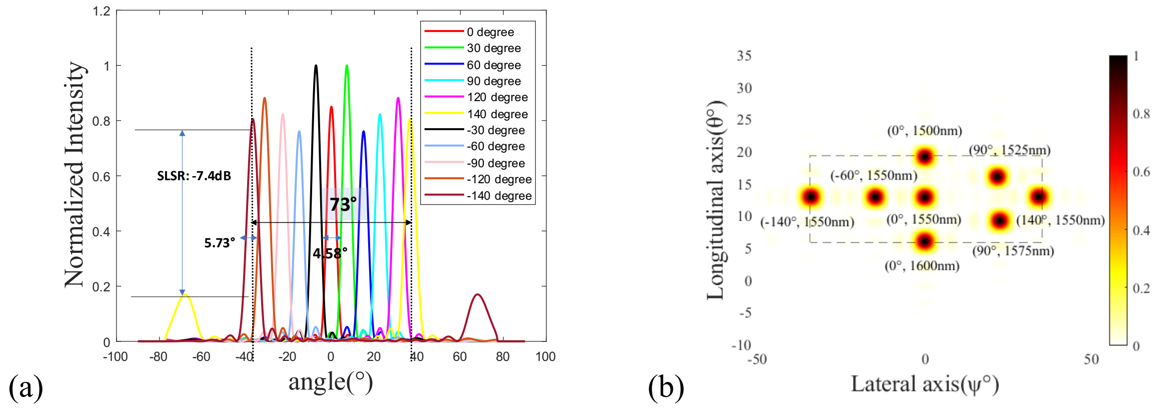

Figure 4. (a): Numerical results of beam steering of superlattice structure by using FDTD method with the phase shift -140° to +140°. (b): 2D beam steering around a 73° × 13.6° FoV.

Conclusion:

The proposed design is a InP-based grating antenna array for 2D beam steering. Here, the superlattice concept is leveraged to achieve low crosstalk and large FoV in lateral steering. For the 17 channels GA array, a 73° of FoV is achieved numerically. This OPA structure on the IMOS platform can potentially achieve high integration density with monolithic active components, which will contribute to a fully-integrated solid-state automotive LiDAR.

References:

[1] C.-P. Hsu *et al.*, 'A Review and Perspective on Optical Phased Array for Automotive LiDAR', *IEEE J. Sel. Top. Quantum Electron.*, vol. 27, no. 1, pp. 1–16, Jan. 2021, doi: 10.1109/JSTQE.2020.3022948.

[2] T. Komljenovic, R. Helkey, L. Coldren, and J. E. Bowers, 'Sparse aperiodic arrays for optical beam forming and LIDAR', *Opt. Express*, vol. 25, no. 3, p. 2511, Feb. 2017, doi: 10.1364/OE.25.002511.

[3] L. Wang *et al.*, 'Design of a low-crosstalk half-wavelength pitch nano-structured silicon waveguide array', *Opt. Lett.*, vol. 44, no. 13, p. 3266, Jul. 2019, doi: 10.1364/OL.44.003266.

[4] G. Zhou, S.-W. Qu, J. Wu, and S. Yang, 'Design of a Low-Crosstalk Sub-Wavelength-Pitch Silicon Waveguide Array for Optical Phased Array', *IEEE Photonics J.*, vol. 13, no. 4, pp. 1–8, Aug. 2021, doi: 10.1109/JPHOT.2021.3103392.

[5] W. Song *et al.*, 'High-density waveguide superlattices with low crosstalk', *Nat. Commun.*, vol. 6, no. 1, p. 7027, Nov. 2015, doi: 10.1038/ncomms8027.

[6] Y. Wang *et al.*, 'InP-Based Grating Antennas for High-Resolution Optical Beam Steering', *IEEE J. Sel. Top. Quantum Electron.*, vol. 27, no. 1, pp. 1–7, Jan. 2021, doi: 10.1109/JSTQE.2019.2958999.

[7] Z. Wu, Q. Huang, J. Xia, and W. Jiang, 'Optical phased array antenna with wide steering range using grating array superlattices', in *Sixth International Conference on Optical and Photonic Engineering (icOPEN 2018)*, Shanghai, China, Jul. 2018, p. 96. doi: 10.1117/12.2500591.

[8] Y. Jiao *et al.*, 'Indium Phosphide Membrane Nanophotonic Integrated Circuits on Silicon', *Phys. Status Solidi A*, vol. 217, no. 3, p. 1900606, Feb. 2020, doi: 10.1002/pssa.201900606.